PAPER

Application of combustion flames for generation of third harmonic and super-hydrophobic coating of glasses by deposited carbon nanoparticle films

To cite this article: G S Boltaev et al 2020 *J. Phys. D: Appl. Phys.* **53** 075301

View the article online for updates and enhancements.

Application of combustion flames for generation of third harmonic and super-hydrophobic coating of glasses by deposited carbon nanoparticle films

G S Boltaev[1] , R A Ganeev[1,2,6] , S Reyimboyev[3], B R Sobirov[3,4],
T Y Shermatov[3], B R Kutlimurotov[3], V V Kim[1], N Y Iskandarov[4],
Z T Azamatov[4], N S Khalilova[5], M Iqbal[1], S A Khan[1] and A S Alnaser[1,6]

[1] Department of Physics, American University of Sharjah, PO Box 26666, Sharjah, United Arab Emirates
[2] Faculty of Physics, Voronezh State University, 1 University Square, Voronezh 394006, Russia
[3] Institute of Ion-Plasma and Laser Technologies, Uzbek Academy of Sciences, Tashkent 100125, Uzbekistan
[4] Centre of Advanced Technology, Innovation Ministry of Uzbekistan, Tashkent 100174, Uzbekistan
[5] Tashkent University of Information Technologies named after Muhammad Al-Khwarizmi, Tashkent 100200, Uzbekistan

E-mail: rashid_ganeev@mail.ru and aalnaser@aus.edu

CrossMark

Abstract

We analyzed the third harmonic generation (THG) of 1064 nm, 28 ps radiation in the candle and ethanol flames. The formation of soot nanoparticles in the candle flame led to the increase of third harmonic yield compared to the ethanol flame. 12- and 24-fold enhancement of the third harmonic yield in candle and ethanol flames compared to the THG in air was achieved. The influence of the nonlinear refraction in air and combustion flames on the phase-matching conditions of THG was found responsible for deviation from the cubic $I_{3\omega}(I_\omega)$ dependence. THG conversion efficiencies of Nd:YAG laser radiation were found to be 1×10^{-5}, 1.2×10^{-4} and 2.4×10^{-4} in the cases of air, carbon flame and ethanol flame media, respectively. Furthermore, the super-hydrophobic properties of the deposited carbon species from the candle flame were demonstrated.

(Some figures may appear in colour only in the online journal)

1. Introduction

Harmonic generation of laser pulses is a technique allowing the conversion of the visible and infrared radiation toward the ultraviolet (low-order harmonics) [1] and extreme ultraviolet (high-order harmonics) [2] ranges of spectra. Additionally, this technique is useful for generation of attosecond pulses through the high-order harmonic generation [3, 4]. During the last two decades, air and laser-produced plasmas (LPP) were

considered as the suitable media for efficient third harmonic generation (THG). Those studies were aimed to enhance THG conversion efficiency (CE) in air and LPPs [5]. The CE of third harmonic (TH) can be increased by varying a duration, focusing geometry, and energy of driving pulses [6]. The low-excited and low-ionized conditions of LPP have demonstrated high CE towards harmonics generation when compared to highly-excited and highly-ionized plasmas [7]. The decrease of THG CE with the increase of the concentration of free electrons in air was observed in [8]. Relatively efficient (up to 3%) third-harmonic generation of picosecond Nd:YAG laser pulses

---

[6] Authors to whom any correspondence should be addressed.

J. Phys. D: Appl. Phys. **53** (2020) 075301

G S Boltaev *et al*

for wavelength $\lambda = 1064$ nm in a low-density laser plasma was reported in [9]. The produced TH beam was nearly diffraction limited. The coherence of TH was studied as a way for *in situ* determination of the relative phases in multi-color pump for analysis of the nonlinear optical processes [10].

Meanwhile, combustion flames can also be considered as the nonlinear media for *in situ* studies of the correlation between their nonlinear optical properties and composition of the burned material. The combustion flames consisting of carbon-containing species were studied in [11]. It was shown that TH CE in laser-induced filament inside the combustion flame is sensitive to the ellipticity of the driving Ti:sapphire laser pulse, while being not much sensitive to the choice of alcohol species introduced as a fuel for the combustion flames. The analysis of the low-order optical nonlinearities of small-sized metal nanoparticles (NPs) showed the advantages in generating low-order harmonics [12, 13] taking into account the influence of the quantum confinement effect in NPs on their nonlinear optical response [14, 15]. THG showed the notable enhancement when TH emission became matched with the plasmon frequency of NPs.

In this paper, we demonstrate the enhancement of TH in the combustion flames of candle and ethanol compared to the air at the same experimental conditions. THG conversion efficiencies of Nd:YAG laser radiation were found to be 1×10^{-5}, 1.2×10^{-4} and 2.4×10^{-4} in the cases of air, carbon flame and ethanol flame. We also analyze the correlation between the presence of the carbon soot NPs in candle flame as emitters of strong TH and the wettability properties of deposited soot. The deposited debris of carbon-containing materials has demonstrated the super-hydrophobic properties.

2. Experimental arrangements

The picosecond Nd:YAG laser (1064 nm, 28 ps; PL-2250, Ekspla) was used to study THG in air and combustion flames. The scheme of THG in flame at air conditions is presented in the inset of figure 1. 150 mm focal length lens was used for focusing the laser pulses in the center of the combustion flame produced by either burned candle or ethanol. The beam waist radius of the focused radiation was 16 μm. The intensity of the driving pulse at the focal plane was varied between 1.0×10^{12} and 3.0×10^{13} W cm^{-2}. The TH (354.6 nm) pulses were separated from the driving radiation (1064 nm) using the color filters and detected by a fiber spectrometer (HR4000, Ocean Optics). We also analyzed the morphology of the films deposited on the nearby substrates during burning of candle and ethanol flames using atomic force microscope (AFM; Solar Next, NT-MDT). The drop-shape analyzer (DSA100-E, Krüss) was used for measurements of the contact angle between the water and the films deposited from the candle flame. The spatial distribution of TH was imaged using CCD camera (Pulnix TM-1020-15CL).

The details of the soot collection were as follow. We placed the glass slide approximately 50 mm above the flame center. The collection of deposited soot particles was lasted during 1 to 10 min to form the layer sufficient for wettability
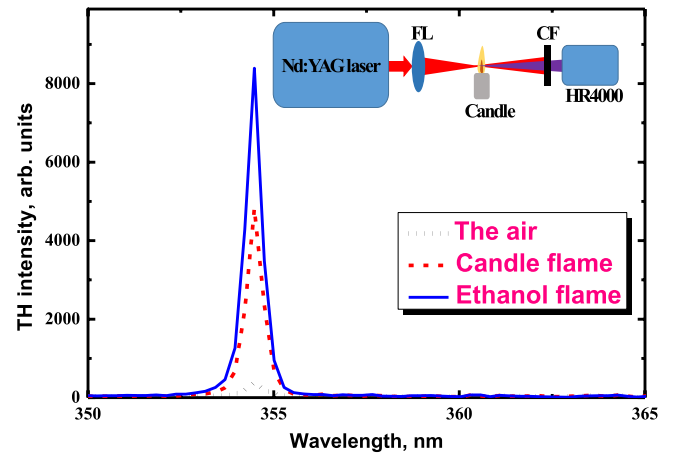
Figure 1. Comparative TH spectra generated in air (dotted curve), candle flame (dashed curve) and ethanol flame (solid curve). In all cases, the energy of 1064 nm pulses was maintained at 3.6 mJ. Inset: experimental setup of THG in combustion flames: FL, focusing lens; CF, color filter; HR4000, fiber spectrometer.

measurements. Important parameters of deposited films are the morphology, structure and thickness. The thickness of film was varied in the range of 1–15 μm. This variation was depended on the number of laser shots at THG experiments during which the deposition was carried out.

3. Results and discussion

Figure 1 presents the TH spectra generated in the flames of candle and ethanol, as well as in air. The twelve-fold enhancement of TH efficiency in the case candle flame and twenty four-fold enhancement in case of ethanol flame were obtained with regard to the TH in air. THG conversion efficiencies of Nd:YAG laser radiation were measured to be 1×10^{-5}, 1.2×10^{-4} and 2.4×10^{-4} in the case of air, carbon flame and ethanol flame, respectively. We considered air as a nonlinear medium which consisted on the mixture of different components (N$_2$, O$_2$, Ar). The typical component of candle is a hydrocarbon of the paraffin wax (C$_{31}$H$_{64}$). Since the TH CE from the gases was 12 and 24 times smaller than from the flames we did not take into account the separate involvement of those air components in the TH studies reported in the present paper.

We assumed that NPs could be responsible for the observed amendment of TH efficiency in the case of combustion flames with regard to the air. THG is based on the third-order nonlinear response of the media. There is a small probability in the presence of NPs in air. Meanwhile, in the case of flames, the formation of NPs is anticipated during the combustion process.

The indirect confirmation for this process is the appearance of NPs in the debris. Earlier, it was suggested that the presence of NPs in such plasma plumes may increase the high-order harmonic CE [11]. An analogous tendency has earlier been reported in the cases of indium and manganese plasmas [5]. The maximum TH efficiency (~10^{-4}) was achieved in the case of the manganese plasma.
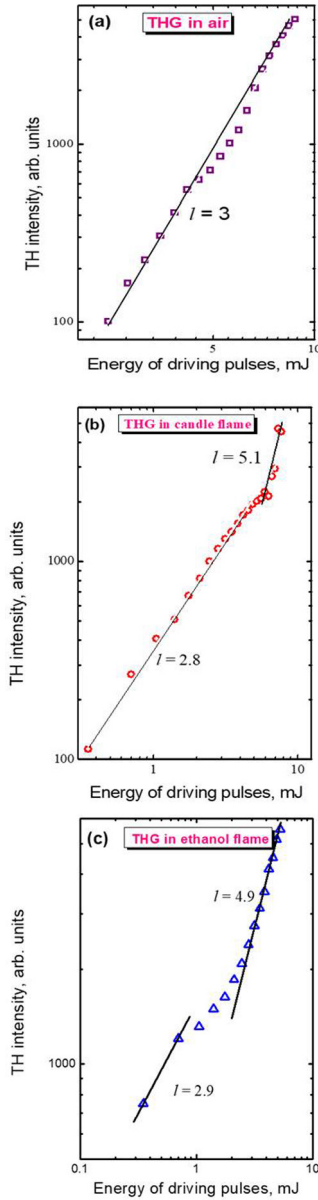
Figure 2. The dependences of TH intensity on the energy of driving 1064 nm, 28 ps pulses in the case of (a) air, (b) candle flame, and (c) ethanol flame.

We analyzed TH from the flames that contain the soot NPs and ethanol molecules. The dependence of TH yield on the driving pulse energy is an important parameter to determine the restricting mechanisms of this process.

Figure 2 shows these dependences of the intensities of TH at different energies of driving pulses in air, candle flame, and ethanol flame. Some small saturation of TH yield was observed in the case of air, which led to insignificant deviation of the slope of this dependence from the anticipated $l = 3$ at the highest used pulse energies. This behavior can be explained by the growing concentration of the free electrons in air at the highest intensity of driving pulses. The dependence of the TH yield on the free electrons concentration has early been reported in [9]. In our experiments, the stronger saturation of TH intensity (I_{TH}) with the growth of laser energy (E) was

observed in cases of ethanol and candle flames, which was further modified by larger slopes of $I_{TH}(E)$ dependences ($I_{TH} \sim E^5$, figures 2(b) and (c)).

One of the mechanisms responsible for the saturation of $I_{TH} \sim E^3$, leading to smaller slope of this dependence can be the phase shift caused by the influence of Kerr nonlinearities [6, 16, 17]. Meanwhile, the unusual $I_{TH} \propto E^5$ dependence can be explained by second-order Kerr effect. In order to achieve the phase-matching conditions during THG in the case of plane waves interactions, the relation $\Delta k = k_3 - 3k_1 = 0$ (where k_1 and k_3 are the wave vectors of the driving and harmonic radiation) has to be fulfilled. This condition ($\Delta k = 0$) is realized in the case when the frequency of generated harmonic is located in the region of anomalous dispersion of the investigated medium [18, 19]. Both air and used flames possess a normal dispersion in the region of $\lambda = 354.6$ nm. Therefore, the phase-matching condition was not fulfilled for the observed process. The intensity of generated TH radiation in that case can be estimated in accordance to [20]:

$$I_{3\omega} = \gamma^2 l^2 I_{10}^3 \exp(-6k_1 r^2/b)\frac{\sin^2\Delta(l,r)}{\Delta^2(l,r)} \quad (1)$$

where $\gamma = 24\pi^3\chi^{(3)}(-3\omega;\omega,\omega,\omega)/(n_1^{3/2}n_3^{3/2}c\lambda_1)$, $\Delta(l,r) = 2b/l - \alpha - \beta$, $\alpha = 2l\Delta k$ is the normalized phase-mismatching, $\beta = 72\pi^3 l\Delta\chi_k I_{10}\exp(-2k_1 r^2/b)/(n_1^2 c\lambda_1)$, $\Delta\chi_k = \chi^{(3)}(-\omega;\omega,\omega,-\omega)/2 - n_1\chi^{(3)}(-3\omega;3\omega,\omega,-\omega)/n_3$ is the difference of Kerr-induced nonlinearities, responsible for refraction indices changes at the wavelengths of fundamental radiation and harmonic, λ_i, k_i and n_i are the wavelengths, wave numbers and refraction indices on the frequency of *i*-radiation, I_{10} is the maximal intensity at the plane of beam waist, b is the confocal parameter of the focused driving radiation, and l is the thickness of nonlinear medium.

The above equation depicting the relation between the intensities of TH and driving radiation ($I_{3\omega} \propto I_{1\omega}^3$) is fulfilled at respectively low influence of self-interaction effects ($|\beta| \ll b/l$) that lead to the phase-mismatch of the interacting waves. For calculation of THG at stronger influence of self-interaction, one has to apply more complicated equations, that would take into account the variations of the wave fronts of interacted radiations (effects of self-focusing and self-defocusing) [21]. It was shown in [21] that, in the case of the influence of Kerr effect, the variations of medium's optical properties change the spatial parameters of the focused beam, which leads to possibility of THG in the medium possessing normal dispersion. The calculations have shown that the slope of the intensity dependence of harmonic yield changes from cubic to fifth order.

Our studies of combustion flames showed qualitative similarity between the anticipated theoretical dependence and experimental data at larger energies of laser pulses ($I_{3\omega} \propto I_{1\omega}^5$). The theoretical calculations [20] have shown that, with further growth of laser intensity, one can anticipate a notable decrease of the slope of this dependence. The THG CE in that case does not exceed 1.3×10^{-3} in accordance with the calculations of relations [19] for weak focusing at
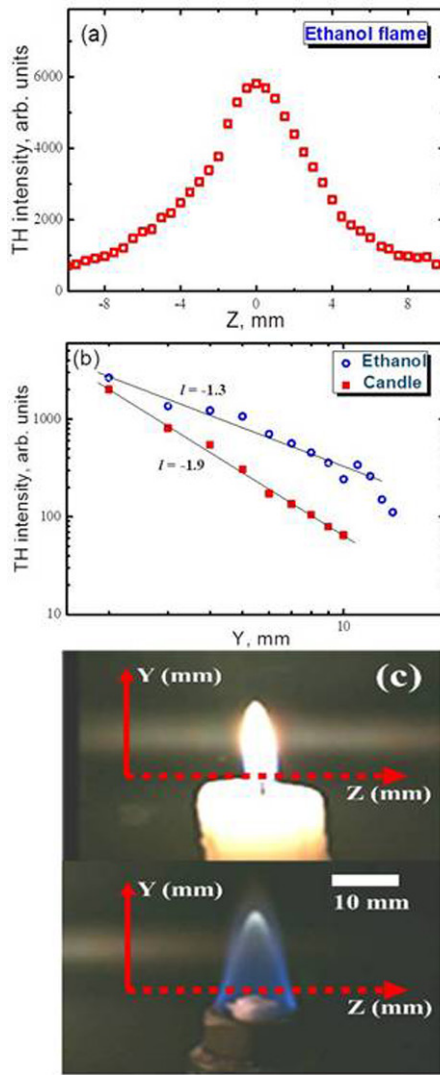
Figure 3. (a) Variation of TH intensity on the position of ethanol flame with regard to the focal plane of focusing lens. (b) Dependence of TH yields on the distance from the base of ethanol (empty circles) and candle (filled squares) flames. (c) Raw images of candle (upper panel) and ethanol (bottom panel) flames. The height of flames was equal to 20 mm. The widths of the flames were estimated to be about 6 and 10 mm for the candle and ethanol flames, respectively.

the center of nonlinear medium. Our experimental results of maximal CE (2.4×10^{-4}) were approximately 5 times below the maximally estimated efficiency of this process.

We analyzed the influence of the position of samples with regard to the focal plane of the focusing lens. Those measurements were carried out by moving the candle and ethanol flames along the z and y axes. In the case of z-scans, i.e. measurements of the harmonic yield as a function of the position z of the focus of the driving laser with regard to the center of the ethanol flame, the maximal TH yield was observed at the position of the flames close to the focal plane of the focusing lens (figure 3(a)).

The measurements along the y axis, i.e. distance from the base of flame to the end of the flame perpendicular to the propagation direction of the driving pulses, showed the anticipated monotonic decrease of TH yield (figure 3(b)). We observed
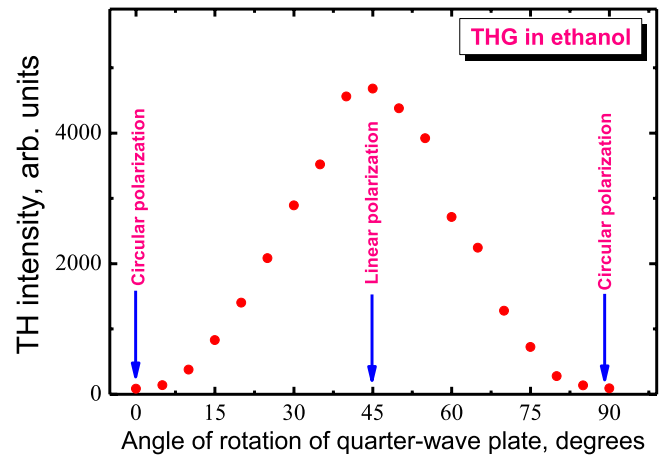
Figure 4. The dependence of the intensity of the TH generating in the ethanol flame on the driving pulses polarization.

different slopes ($l = -1.3$ and $l = -1.9$) of TH curves for the candle and ethanol flames, respectively. In the case of candle flame, the decrease of the TH yield along the y axis can be explained by a decrease of the concentration of the NPs produced during burning of the candle flames. The evolution of soot NPs formation was analyzed in [22]. The comparison of primary particle and aggregate sizes between the centerline and other streamlines suggested that the evolution processes of particles formation in different parts of the flame are different. In the case of ethanol flame, the probability of aggregation of particles is smaller than in the case of candle flame that was confirmed by the analysis of the deposited films from flames. In the case of ethanol flame, we did not observe a large amount of deposited debris on the nearby glass substrate. The decrease of TH yield from ethanol flame is related with the decrease of the concentration of particles due to the expansion of ethanol flame in air.

Figure 4 shows the variation of TH intensity at different polarizations of the driving picosecond pulses propagating through the ethanol flame. This curve was measured at different angles of rotation of the quarter-wave plate installed in front of the focusing lens. The rotation of plate caused the variation of the polarization of driving radiation from linear (at the angle of rotation of 45°) to circular (at 0° and 90°). Figure 4 demonstrates a decrease of TH intensity when the polarization of the driving pulses deviates from the linear polarization. This dependence is a characteristic of the nonlinear optical frequency conversion in any isotropic medium. The application of circularly polarized laser pulses led to the complete disappearance of TH emission.

We also analyzed the spatial distributions of TH beams generated in air, candle flame and ethanol flame. The Gaussian profile of driving beam was converted to the TH beam with insignificant wave-front distortion. The spatial distributions of the TH beam generated in air, candle flame and ethanol flame are shown in figure 5. We observed the Gaussian-like profiles of the TH beams generated in three media at similar experimental conditions. The different brightness of the spatial distribution of TH was due to the difference in the CEs of the third-order nonlinear optical process in these three media. The

J. Phys. D: Appl. Phys. **53** (2020) 075301

G S Boltaev *et al*
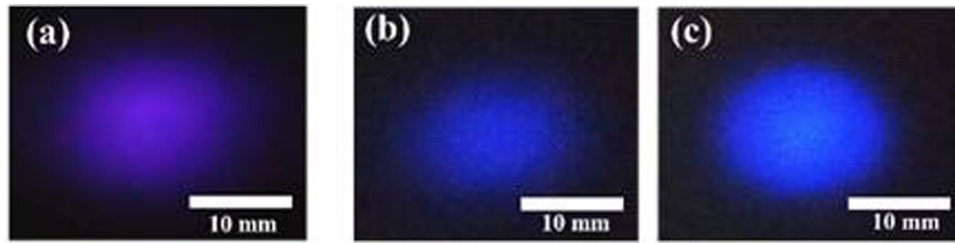
Figure 5. Spatial distributions of the TH beams ($\lambda = 355$ nm) generated in (a) air, (b) candle flame, and (c) ethanol flame using the 3.5 mJ driving pulses.
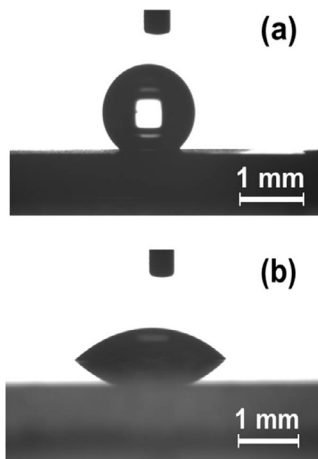
Figure 6. (a) Raw image of the deposited soot from candle flame, which demonstrated the super-hydrophobic properties with 155° contact angle. (b) The hydrophilic properties of water on the surfaces of non-deposited glass substrates with 36° contact angle.

Figure 7. AFM image of deposited debris.

spatial distribution of TH generated in air using femtosecond pulses has been studied in [23]. The far-field patterns of harmonic emission analyzed in [23] have shown that the output TH pulse splits into an on-axis part and an off-axis conical ring emission due to the tight-focusing geometry and strong influence of the Kerr-induced processes.

In the case of candle flame, some components of this medium (for example, large NPs and aggregates) may, to some extent, modify the phase front of propagating radiation, which in turn causes the spatial modulation of generating TH emission. The debris from the candle and ethanol flames may provide some information about the properties of flame components as the emitters of TH. These properties of deposited materials can also be analyzed by different methods to determine, for example, their hydrophilic and hydrophobic properties. Particularly, the super-hydrophobic properties of the films deposited from candle flames have been discussed in [24]. In [24], the contact angle and roll-off angle were measured as 142° and 6°, respectively.

We used the drop-shape analyzer for the contact angle measurement of the water-surface system. The analysis of the deposited films from the combustion flame produced by the candle is shown in figure 6. We deposited these films during THG on the surfaces of glass substrates. In our case the contact angle was measured to be 155°, i.e. the soot films on the glass substrate demonstrated even stronger super-hydrophobic properties than those reported in [24]. On the other hand,

non-deposited glass substrate showed the hydrophilic properties with 36° contact angle. We observed the small change of the contact angle depending on the thickness of deposited soot film. In the case of ethanol flame, we did not see any change of contact angle due to the notably smaller thickness of deposited film compared with the candle flame.

We also carried out the morphology measurements using AFM. In figure 7, we present the microphotography of the deposited debris from burned candle, which demonstrates the evidence of the presence of NPs in flame. We analyzed AFM images and determined that the size distribution of NPs was varied in different parts of deposited film. Though in some cases we saw a few large NPs (i.e. in the range above 100 nm and below 200 nm), the mean size of NPs was 40 nm and the size distribution was 5–70 nm. Previous studies of the candle flames using different microscopic and spectroscopic methods have also shown the presence of approximately similar NPs among the deposited materials [25–27].

The presence of the soot NPs in the flames causes the enhancement of TH yield. The evidence of the presence of carbon NPs in deposited films proves their presence in the flame. The enhanced TH emission from the plasmas containing NPs has also been analyzed in [28], where the contribution of small-sized carbon NPs to the growth of TH CE has been demonstrated. Our studies showed the coincidence of the enhanced TH yield in the carbon NP-contained medium and the drastic variation of the hydrophobic to super-hydrophobic properties of the carbon NP films deposited from candle flame on the nearby glass surface.

It would be extremely useful to know which group of NPs possessing different sizes is mostly preferable for the growth of the efficiency of this nonlinear optical process. However,

J. Phys. D: Appl. Phys. 53 (2020) 075301

G S Boltaev et al

during these studies it was difficult to separately distinguish the harmonic yield from 1 to 5 nm NPs, 10–30 nm NPs, 40–80 nm NPs, etc. The whole effect of NPs in our studies comprised a summation of the harmonic yields from different groups of NPs. Recent studies pointed out the role of quantum dots possessing the sizes in the range above 1 nm and below 5 nm in the growth of high-order harmonic generation [29]. Probably, the growth of TH yield due to the confinement effect and local field enhancement can also be efficiently manifested in the case of this group of particles.

The correlation of TH conversion efficiency and particles sizes can be qualitatively explained by analyzing figure 3(b). In this figure, we showed the dependences of TH yield on the distance from the base of ethanol (empty circles) and candle (filled squares) flames. Notice that soot NPs formation is a kinetically governed process leading to the change of particle sizes [30].

The studied two processes, i.e. variations of wettability and nonlinear optical frequency conversion, are both relevant with the formation of the small-sized soot NPs in candle flames. The enhanced third-order nonlinear optical response of NPs causes the enhancement of TH yield in the flames of the candle and ethanol. The presence of clusters in the flames was discussed in [31], where the feasibility for combustion diagnostics of flames using femtosecond filament excitation was demonstrated. The soot as a representative of carbon-based materials contains an abundant of nanomaterials, which have earlier demonstrated the advantages over graphite and carbon nanotubes as the efficient emitters of harmonics.

The enhancement factor of TH emission depended on the presence of the smallest NPs appearing during the burning of the candle. During these studies, we demonstrated the possibility of soot NPs to generate strong low-order harmonic and to form a coating, which allowed varying the wettability contact angle of the substrate. The wettability properties of these deposited structures were depended on the roughness of the substrates and on the presence of the nano- or microstructures of deposited carbon-contained species. Thus, our studies revealed that the candle flame can both create the preferable conditions for THG and produce the deposited layers of soot allowing modification of the contact angle for water drop.

4. Conclusions

In these studies, the main attention was focused on the enhancement of conversion efficiency of the third-harmonic generation in combustion flames using 25 ps, 1064 nm driving pulses. We demonstrated that the enhancement of TH intensity is attributed to the formation of carbon-containing NPs. In the meantime, we have shown that the roughness of deposited surfaces is an important factor in the modification of the wetting properties of substrates. AFM measurements allowed analyzing the deposited surface morphology to determine the correlation between the modified hydrophobic properties of formed surfaces and the structure of the modified flat glass substrates during soot deposition.

We have analyzed the nonlinear optical and wettability properties of different combustion flames and their debris. We have demonstrated the enhancement of TH yield from the candle and ethanol flames compared with TH in air using 1064 nm, 28 ps pulses and attributed the enhancement of this process in the former media to the influence of small-sized structures. The 12- and 24-fold enhancement of the TH yield in candle and ethanol flames compared with the THG in air was achieved. An influence of the nonlinear refraction in the air and combustion flames on the phase-matching conditions of THG was responsible for deviation from the cubic $I_{3\omega}(I_\omega)$ dependences. THG conversion efficiencies of Nd:YAG laser radiation were found to be 1×10^{-5}, 1.2×10^{-4} and 2.4×10^{-4} in the cases of air, carbon flame and ethanol flame. The deposited debris of carbon-containing materials on the glass substrate has demonstrated the super-hydrophobic properties with 155° contact angle of water drop.

ORCID iDs

G S Boltaev ⬥ https://orcid.org/0000-0003-0354-1251
R A Ganeev ⬥ https://orcid.org/0000-0001-5522-1802

References

[1] Aközbek N, Iwasaki A, Becker A, Scalora M, Chin S L and Bowden C M 2002 *Phys. Rev. Lett.* **89** 143901
[2] Lewenstein M, Balcou P, Ivanov M Yu, L'Huillier A and Corkum P 1994 *Phys. Rev.* A **49** 2117
[3] Corkum P and Krausz F 2007 *Nat. Phys.* **3** 381
[4] Krausz F and Ivanov M 2009 *Rev. Mod. Phys.* **81** 163
[5] Ganeev R A, Boltaev G S, Tugushev R I, Usmanov T, Baba M and Kuroda H 2010 *J. Opt.* **12** 055202
[6] López-Arias M, Oujja M, Sanz M, Ganeev R A, Boltaev G S, Satlikov N Kh, Tugushev R I, Usmanov T and Castillejo M 2012 *J. Appl. Phys.* **111** 043111
[7] Ganeev R A, Suzuki M, Baba M, Kuroda H and Kulagin I A 2006 *Appl. Opt.* **45** 748–55
[8] Rodríguez C, Sun Z, Wang Z and Rudolph W 2011 *Opt. Express* **19** 16115
[9] Fedotov A B, Gladkov S M, Koroteev N I and Zheltikov A M 1991 *J. Opt. Soc. Am.* B **8** 363
[10] Chen W-J, Lin R-Y, Chen W-F, Lee C-K and Pan C-L 2013 *Laser Phys. Lett.* **10** 065401
[11] Zang H-W, Li H-L, Su Y, Fu Y, Hou M-Y, Baltuška A, Yamanouchi K and Xu H 2018 *Opt. Lett.* **43** 615
[12] Boltaev G S, Ganeev R A, Krishnendu P S, Maurya S K, Redkin P V, Rao K S, Zhang K and Guo Ch 2018 *Appl. Phys.* A **124** 766
[13] Melik-Gaykazyan E V *et al* 2017 *ACS Photonics* **5** 728
[14] Lippitz M, van Dijk M A and Orrit M 2005 *Nano Lett.* **5** 799
[15] Liu T-M, Tai Sh-P, Yu Ch-H, Wen Y-Ch and Chu Sh-W 2006 *Appl. Phys. Lett.* **89** 043122
[16] Boltaev G S, Ganeev R A, Kulagin I A and Usmanov T 2014 *J. Opt. Soc. Am.* B **31** 436
[17] Theobald W, Wűlker C, Schäfer F R and Chichkov B N 1995 *Opt. Commun.* **120** 177
[18] Bjorklund G 1975 *IEEE J. Quantum Electron.* **11** 285

J. Phys. D: Appl. Phys. **53** (2020) 075301

G S Boltaev *et al*

[19] Reintjes J F 1984 *Nonlinear Optical Parametric Processes in Liquids and Gases* (Academic: New York)

[20] Kulagin I A and Usmanov T 1998 *Quantum Electron.* **28** 1092

[21] Ganeev R A, Gorbushin V V, Kulagin I A and Usmanov T 1996 *Appl. Phys.* B **41** 69

[22] Kholghy M, Saffaripour M, Yip C and Thomson M J 2013 *Combust. Flame* **160** 2119

[23] Xu H, Xiong H, Li R, Cheng Y, Xu Z and Chin S L 2008 *Appl. Phys. Lett.* **92** 011111

[24] Zhao L, Zhao K, Yan W-G and Liu Z 2018 *Materials* **11** 2318

[25] Barone A 2003 *Combust. Flame* **132** 181

[26] Sgro L, Basile G, Barone A, D'Anna A, Minutolo P, Borghese A and D'Alessio A 2003 *Chemosphere* **51** 1079

[27] Lamprecht A, Eimer W and Höinghaus K K 1999 *Combust. Flame* **118** 140

[28] Singh R P, Gupta S L and Thareja R K 2015 *Phys. Plasmas* **22** 123302

[29] Ganeev R A *et al* 2018 *Opt. Express* **26** 35013

[30] Sahoo B N and Kandasubramanian B 2014 *Mater. Chem. Phys.* **148** 134

[31] Li H L, Xu H L, Yang B S, Chen Q D, Zhang T and Sun H B 2013 *Opt. Lett.* **38** 1250